Rare Metal Materials and Engineering
Volume 53, Issue 1, January 2024
Available online at www.rmme.ac.cn

Science Press

Cite this article as: Peng Zhen, Guo Qingyu, Sun Jian, et al. Effect of Mo Addition on Tribological Properties of $Al_{19}Fe_{20-x}Co_{20-x}Ni_{41}Mo_{2x}$ Eutectic High-Entropy Alloys[J]. Rare Metal Materials and Engineering, 2024, 53(01): 17-22. DOI: 10.12442/j.issn.1002-185X.E20230033.

ARTICLE

Effect of Mo Addition on Tribological Properties of $Al_{19}Fe_{20-x}Co_{20-x}Ni_{41}Mo_{2x}$ Eutectic High-Entropy Alloys

Peng Zhen[1], Guo Qingyu[1], Sun Jian[1], Li Keran[2], Luan Hengwei[3,4,5], Gong Pan[2,6]

[1] School of Materials Science and Engineering, Jiangsu University, Zhenjiang 212013, China; [2] School of Materials Science and Engineering, Huazhong University of Science and Technology, Wuhan 430074, China; [3] Department of Mechanical Engineering, City University of Hong Kong, Hong Kong 999077, China; [4] Hong Kong Branch of National Precious Metals Material Engineering Research Centre, City University of Hong Kong, Hong Kong 999077, China; [5] School of Materials Science and Engineering, Tsinghua University, Beijing 100084, China; [6] Research Institute of Huazhong University of Science and Technology, Shenzhen 518057, China

Abstract: Tribological properties of $Al_{19}Fe_{20-x}Co_{20-x}Ni_{41}Mo_{2x}$ (x=0, 1, 2, 3, 4, 5) eutectic high-entropy alloys (EHEAs) were investigated in this research. Results show that EHEAs with trace Mo addition can form the face-centered cubic (fcc)+B2 eutectic microstructure, whereas EHEAs with relatively higher Mo content can form fcc+B2+μ dendritic microstructure. Mo element is beneficial to the strength enhancement of $L1_2$ phase and the ductility improvement of B2 phase. However, with increasing the Mo content to x>2, the resultant Mo-rich μ phase degrades the strength and plasticity of EHEAs. $Al_{19}Fe_{18}Co_{18}Ni_{41}Mo_4$ EHEA has the optimal combination of high strength and high ductility. Increasing Mo content can improve the oxidation resistance of EHEAs. With increasing the Mo content, EHEA forms a tribo-oxide layer with improved oxidation resistance during sliding process, and the friction coefficient is monotonically decreased. This research provides guidance for the investigation of tribological properties of $Al_{19}Fe_{20-x}Co_{20-x}Ni_{41}Mo_{2x}$ EHEAs.

Key words: eutectic high-entropy alloys; tribological property; strength; plasticity

Combining eutectic alloy with high-entropy alloys (HEAs), the eutectic high-entropy alloys (EHEAs)[1–5] with eutectic microstructure and HEA composition have been proposed, which have many attractive properties, such as excellent mechanical properties[6–9], good wear resistance[10–13], and 3D printability[14–16]. It is reported that the $AlCoCrFeNi_{2.1}$ EHEA has fine lamellar microstructure with optimal combination of strength and ductility, and the additive-manufactured $AlCoCrFeNi_{2.1}$ EHEAs show better mechanical properties than most other additive-manufactured alloys do[14]. The directionally solidified $Al_{19}Fe_{20}Co_{20}Ni_{41}$ EHEA presents herringbone microstructure with a strong crack buffering effect, implying ultra-high uniform tensile elongation without strength degradation[9].

The eutectic microstructure of $Al_{19}Fe_{20}Co_{20}Ni_{41}$ EHEA consists of the ordered face-center cubic (fcc) phase ($L1_2$ phase) and ordered body-centered cubic (bcc) phase (B2 phase). It is found that the Mo addition is beneficial to the strength enhancement of $L1_2$ phase[17] and the ductility improvement of B2 phase[18–19] in the intermetallic compounds. Additionally, the minor addition of Mo element can even ameliorate the oxidation resistance by forming a dense and continuous oxide scale during high-temperature oxidation[20]. Therefore, the $Al_{19}Fe_{20}Co_{20}Ni_{41}$ EHEAs with Mo addition show great potential as structural materials.

Tribological performance is an important mechanical property for structural materials. It is reported that the formation of eutectic lamellar microstructure is beneficial to increase the hardness, thereby improving the wear resistance[21–27]. Besides, the oxidation resistance can be improved by the minor addition of Mo element in the $Al_{19}Fe_{20}Co_{20}Ni_{41}$ EHEA[20], which also contributes to the enhancement in wear resistance. Therefore, in this research, a series of $Al_{19}Fe_{20}$-

Received date: September 12, 2023
Foundation item: National Natural Science Foundation of China (52271147, 12261160364, 52371154); Guangdong Basic and Applied Basic Research Foundation (2023A1515012158)
Corresponding author: Peng Zhen, Ph. D., Professor, School of Materials Science and Engineering, Jiangsu University, Zhenjiang 212013, P. R. China, Tel: 0086-511-88780190, E-mail: peng@ujs.edu.cn

$Co_{20}Ni_{41}$ EHEAs with Mo addition were prepared to investigate their tribological properties.

1 Experiment

The $Al_{19}Fe_{20-x}Co_{20-x}Ni_{41}Mo_{2x}$ EHEAs with x=0, 1, 2, 3, 4, and 5 (at%) were denoted as Mo_0, Mo_2, Mo_4, Mo_6, Mo_8, and Mo_{10} specimens, respectively. These EHEAs were synthesized by vacuum arc melting in furnace under high-purity argon protection. The purity of all raw materials was above 99.99%. The raw materials were put into the water-cooled copper hearth and remelted at least six times to ensure the chemical homogeneity. The mass of each alloy ingot is about 25 g and the central part of the ingot was selected for analysis. The specimens were cut by the electric discharge machine wire cutter into the ones with size of 5 mm×5 mm×5 mm. All specimens were ground by SiC sandpaper (2000#) and cleaned by ethanol through the ultrasonic cleaner.

The phase structure analysis was conducted through Rigaku SMARTLAB9 X-ray diffractometer (XRD, 40 kV, 150 mA). The morphology and composition were investigated by FEI Nova Nano 450 scanning electron microscope (SEM) coupled with energy dispersive spectrometer (EDS). Compression tests were conducted by AG-X Plus 250 kN/50 kN universal testing machine under deformation rate of 2 and 0.5 mm/min at room temperature. The reciprocating dry friction tests were conducted at room temperature (25 °C). The Si_3N_4 ceramic balls with 5 mm in diameter were used as the friction pair, the friction load was 5 N, the friction amplitude was 5 mm, the friction frequency was 2 Hz (linear velocity was 0.02 m/s), and the test duration was 30 min. Before tests, the alloy surface was polished. The wear morphology was observed by SEM.

2 Results and Discussion

2.1 Microstructure analysis

Mo has a negative binary enthalpy of mixing and relatively low valence electron concentration (VEC), compared with other constitutional elements. Fig. 1 shows the VEC values, mixing enthalpy ΔH_{mix}, mixing entropy ΔS_{mix}, and atomic size difference δ of the $Al_{19}Fe_{20-x}Co_{20-x}Ni_{41}Mo_{2x}$ (x=0, 1, 2, 3, 4, 5) EHEAs. It can be seen that with increasing the Mo content, the mixing enthalpy ΔH_{mix}, mixing entropy ΔS_{mix}, and atomic size difference δ are increased, whereas VEC value is decreased. Hence, the microstructure and phase stability of $Al_{19}Fe_{20-x}Co_{20-x}Ni_{41}Mo_{2x}$ EHEAs may be changed with the composition variation. With increasing the Mo content, the $Al_{19}Fe_{20-x}Co_{20-x}Ni_{41}Mo_{2x}$ EHEAs have relatively large atomic size difference. Based on the solid-solution phase formation rules of HEAs, with increasing the Mo content, the ordered phase tends to precipitate in the solid solution, such as the intermetallic compounds in the matrix[28]. The minimum VEC value is still greater than 8, indicating that the phase composition of $Al_{19}Fe_{20-x}Co_{20-x}Ni_{41}Mo_{2x}$ EHEAs is mainly composed of fcc phase[29].

Fig. 2 shows XRD patterns of $Al_{19}Fe_{20-x}Co_{20-x}Ni_{41}Mo_{2x}$ EHEAs with x=0, 1, 2, 3, 4, 5. It can be seen that the as-prepared Mo_0 EHEA is composed of B2+fcc dual-phase microstructure[20], which is very similar to the B2+$L1_2$ phase[9]. The fcc phase is disordered, because the (100) diffraction peak cannot be observed. With the Mo addition, the B2+fcc dual-phase microstructure remains in the Mo_2 and Mo_4 EHEAs, suggesting that the minor Mo can be dissolved into the dual-phase microstructure. When the Mo content is higher than 4at% (x>2), the μ phase can be observed in the Mo_6 EHEA, and the peak intensity of μ phase is increased with further increasing the Mo addition. The variation in peak intensities of fcc and B2 phases is probably caused by the texture difference of the tested specimens. The results of the microstructure characterization of $Al_{19}Fe_{20-x}Co_{20-x}Ni_{41}Mo_{2x}$ EHEAs are in good agreement with the calculated results, inferring that the solid-solution phase formation rules of HEAs are suitable to predict the phase composition of $Al_{19}Fe_{20-x}Co_{20-x}Ni_{41}Mo_{2x}$ EHEAs.

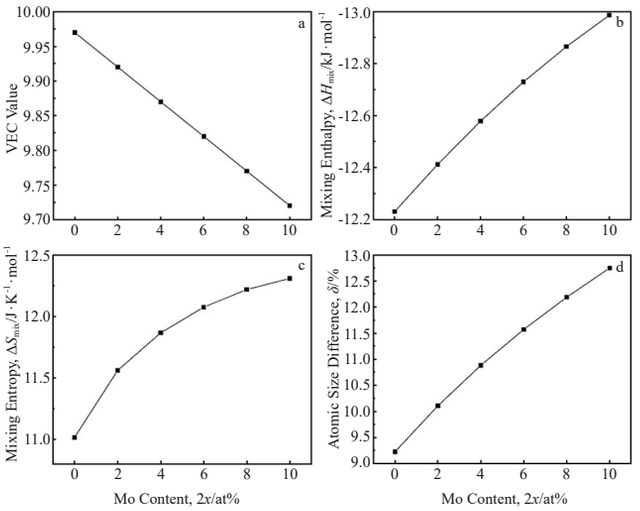

Fig.1 Calculated VEC value (a), mixing enthalpy ΔH_{mix} (b), mixing entropy ΔS_{mix} (c), and atomic size difference δ (d) of different $Al_{19}Fe_{20-x}Co_{20-x}Ni_{41}Mo_{2x}$ EHEAs

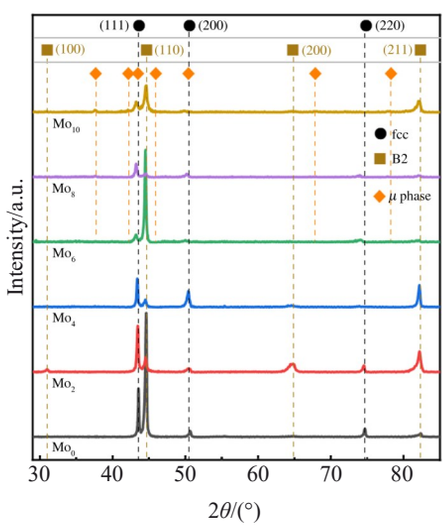

Fig.2 XRD patterns of different $Al_{19}Fe_{20-x}Co_{20-x}Ni_{41}Mo_{2x}$ EHEAs

Fig.3 and Table 1 show SEM morphologies and EDS point analysis results of $Al_{19}Fe_{20-x}Co_{20-x}Ni_{41}Mo_{2x}$ EHEAs with x=0, 1, 2, 3, 4, 5, respectively. The Mo_0 EHEA specimen presents typical fine eutectic microstructure with interlamellar spacing of approximately 2 μm, which is consistent with the results in Ref.[9]. EDS analysis results show that B2 phase is composed of Al and Ni-rich structures, whereas the fcc phase is composed of Fe and Co-rich structures. With increasing the Mo addition, the microstructure is transformed from the fine lamellar eutectic microstructure to the coarse lamellar microstructure in Mo_2 EHEA specimen, and further to the dendritic microstructure in Mo_4 EHEA specimen. EDS results show that the fcc phase is composed of Mo-rich structures, which is consistent with the result in Ni-Al systems[30]. With further increasing the Mo addition, the dendritic microstructure becomes coarser, and the Mo-rich μ phase can be observed along the phase boundary. The proportion of the μ phase is increased with increasing the Mo addition, and the μ phase separates the fcc and B2 phases in the Mo_8 EHEA specimen. The microstructure suggests that the composition of EHEAs with high Mo addition is different from the that of eutectic compound.

2.2 Mechanical properties

Fig.4 shows the compressive engineering stress-engineering strain curves of the $Al_{19}Fe_{20-x}Co_{20-x}Ni_{41}Mo_{2x}$ EHEAs at room temperature. The mechanical compressive properties of $Al_{19}Fe_{20-x}Co_{20-x}Ni_{41}Mo_{2x}$ EHEAs at room temperature are shown in Table 2. Mo_0 EHEA has the yield strength (σ_s) of 751 MPa, ultimate compressive strength (σ_p) of 2593 MPa, and compressive strain at failure (namely elongation ε_p) of 40.5%, which are all higher than the tensile properties in Ref.[9]. This result indicates the strong tension/compression asymmetry effect. With 2at% Mo addition, the Mo_2 EHEA shows slightly

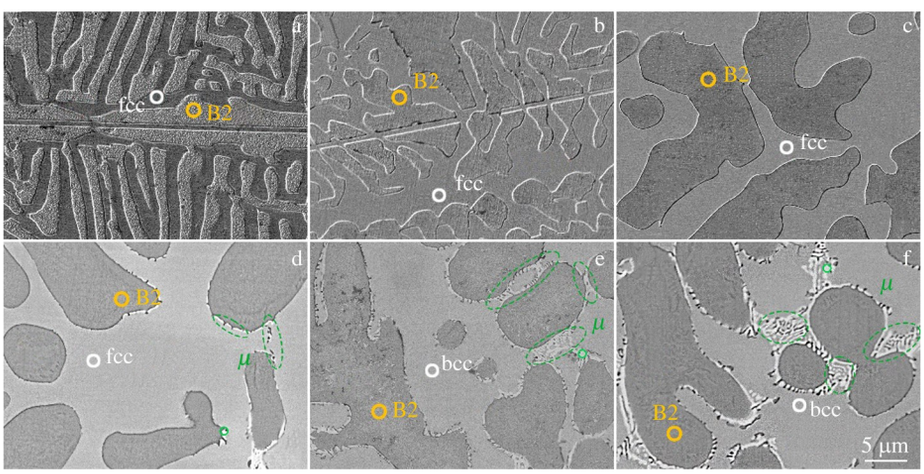

Fig.3 SEM morphologies of different $Al_{19}Fe_{20-x}Co_{20-x}Ni_{41}Mo_{2x}$ EHEAs: (a) x=0; (b) x=1; (c) x=2; (d) x=3; (e) x=4; (f) x=5

Table 1 EDS point analysis results of fcc phase, B2 phase, and μ phase of different $Al_{19}Fe_{20-x}Co_{20-x}Ni_{41}Mo_{2x}$ EHEAs in Fig.3 (at%)

Specimen	Phase	Element				
		Al	Fe	Co	Ni	Mo
Mo_0	fcc	13.72	24.96	20.68	40.64	-
	B2	21.52	19.67	17.53	41.28	-
Mo_2	fcc	11.38	24.03	20.97	40.27	3.35
	B2	25.61	16.54	15.42	42.07	0.36
Mo_4	fcc	10.14	23.94	20.83	40.79	4.29
	B2	22.13	16.70	15.79	44.39	0.99
Mo_6	fcc	10.33	23.83	20.10	37.77	7.97
	B2	21.90	16.32	14.58	44.80	2.40
	μ	5.33	20.91	20.57	24.12	29.07
Mo_8	fcc	12.62	20.41	17.59	37.56	11.82
	B2	24.18	14.15	12.60	45.16	3.91
	μ	6.15	21.88	19.14	24.60	28.23
Mo_{10}	fcc	10.87	22.64	18.89	38.91	8.69
	B2	23.79	15.48	13.50	45.53	1.70
	μ	7.13	21.52	19.43	28.82	23.10

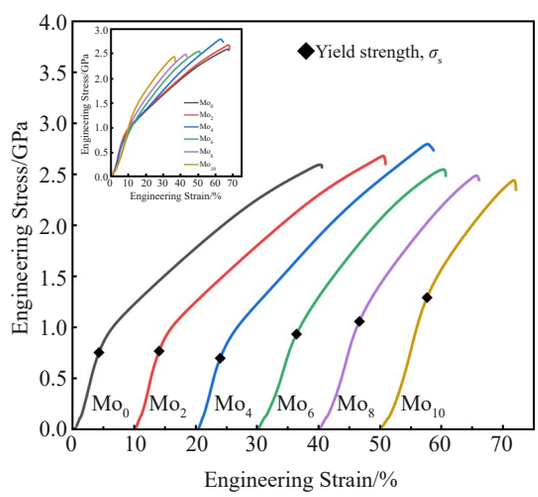

Fig.4 Compressive engineering stress-engineering strain curves of different $Al_{19}Fe_{20-x}Co_{20-x}Ni_{41}Mo_{2x}$ EHEAs

Table 2 Mechanical compressive properties of $Al_{19}Fe_{20-x}Co_{20-x}Ni_{41}Mo_{2x}$ EHEAs near eutectic HEAs at room temperature

Specimen	Yield strength, σ_s/MPa	Ultimate compressive strength, σ_p/MPa	Elongation, ε_p/%
Mo_0	751	2593	40.5
Mo_2	770	2679	40.9
Mo_4	703	2793	39.6
Mo_6	931	2545	30.7
Mo_8	1056	2486	26.1
Mo_{10}	1291	2439	22.1

higher σ_s and σ_p of 770 and 2679 MPa, respectively, and its ε_p value is also slightly increased to 40.9%, inferring the enhancement effect of Mo addition on mechanical properties. The Mo_4 EHEA presents the high σ_p value of 2793 MPa, but its σ_s and ε_p show a slighter decrease. With further increasing the Mo addition, the σ_s value is continuously increased, whereas the σ_p and ε_p values are significantly decreased. This phenomenon is caused by the formation of hard and brittle μ phase along the phase boundary.

2.3 Tribological properties

Fig. 5 shows the coefficient of friction (COF) curves of different $Al_{19}Fe_{20-x}Co_{20-x}Ni_{41}Mo_{2x}$ EHEAs at room temperature. A transition period occurs in the beginning followed by a steady period for all the EHEA specimens, which is consistent with the typical COF curves[31]. With increasing the Mo content, COF is monotonically decreased. Fig. 6 shows the cross-sectional and 3D confocal laser scanning images of the wear tracks of different $Al_{19}Fe_{20-x}Co_{20-x}Ni_{41}Mo_{2x}$ EHEAs. It can

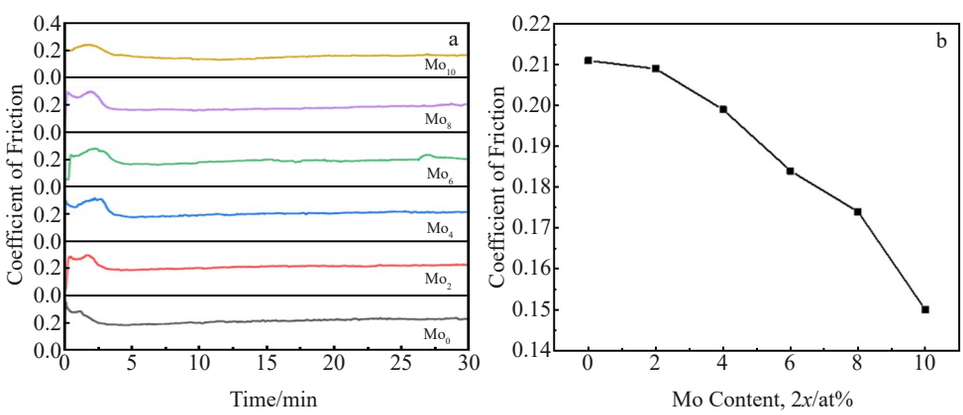

Fig.5 Coefficients of friction of different $Al_{19}Fe_{20-x}Co_{20-x}Ni_{41}Mo_{2x}$ EHEAs

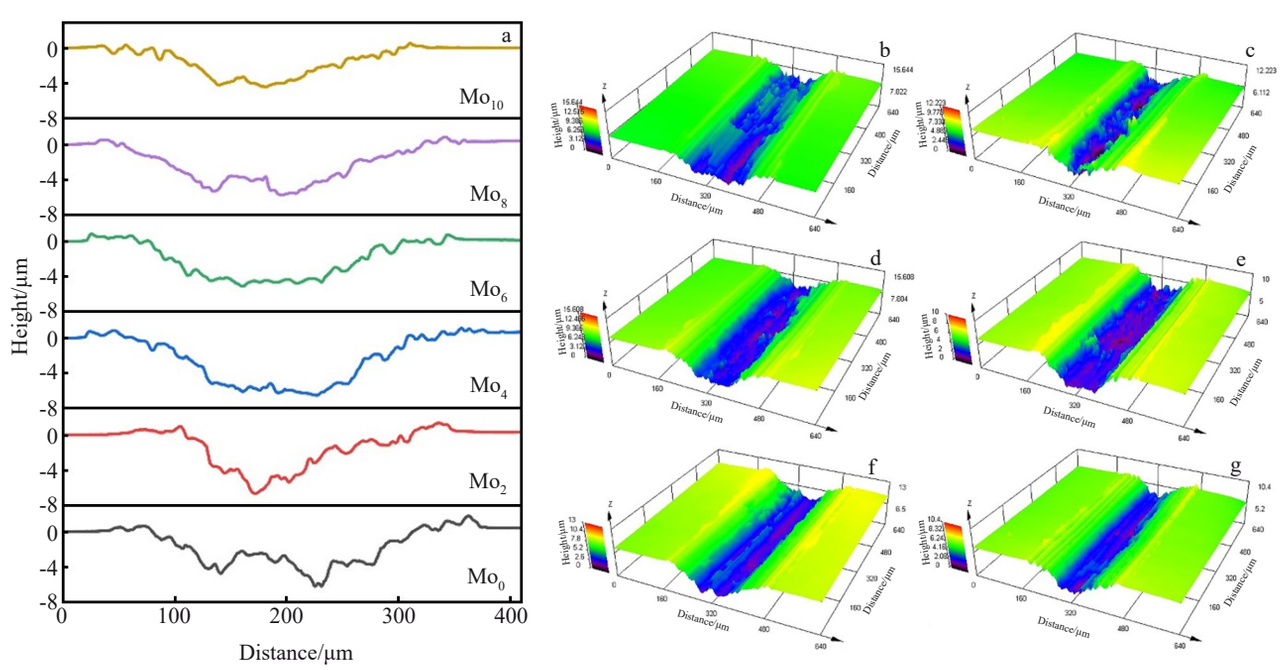

Fig.6 Cross-sectional morphologies (a) and 3D confocal laser scanning images (b–g) of wear tracks of different $Al_{19}Fe_{20-x}Co_{20-x}Ni_{41}Mo_{2x}$ EHEAs: (b) Mo_0; (c) Mo_2; (d) Mo_4; (e) Mo_6; (f) Mo_8; (g) Mo_{10}

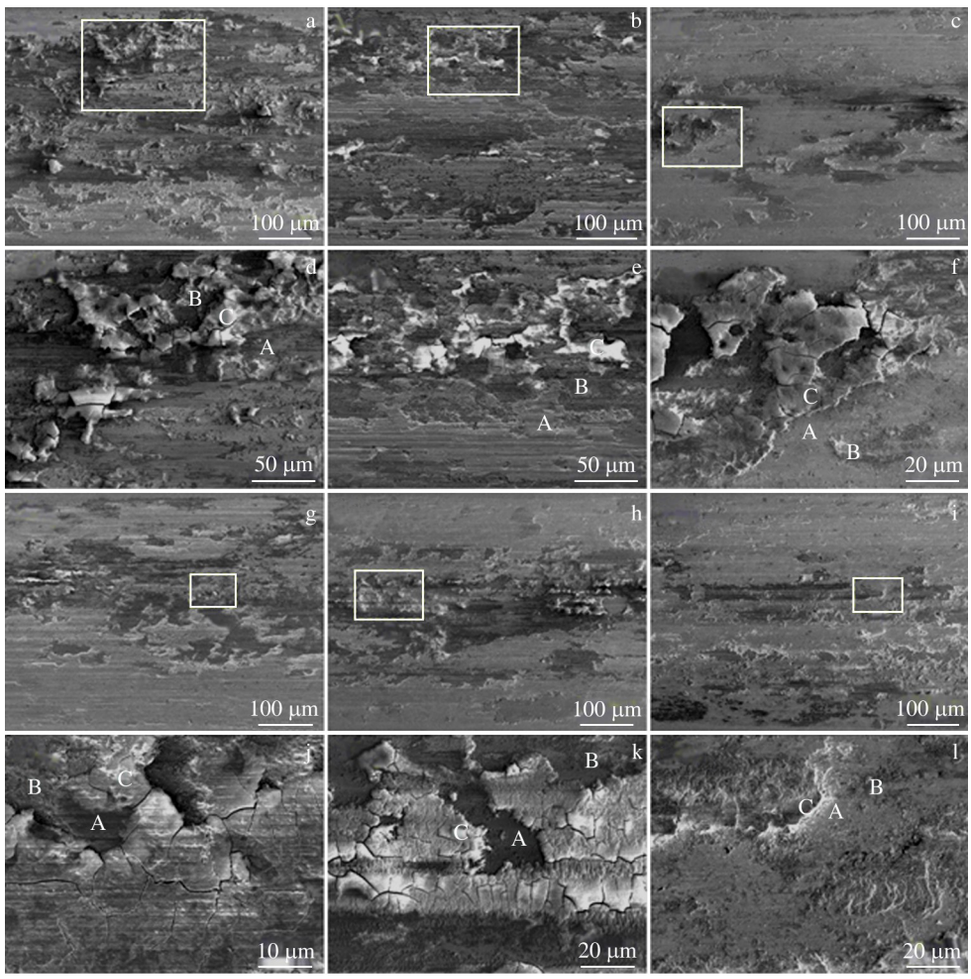

Fig.7 SEM microstructures (a–c, g–i) and magnified images (d–f, j–l) of wear tracks of different $Al_{19}Fe_{20-x}Co_{20-x}Ni_{41}Mo_{2x}$ EHEAs: (a, d) Mo_0; (b, e) Mo_2; (c, f) Mo_4; (g, j) Mo_6; (h, k) Mo_8; (i, l) Mo_{10}

be seen that Mo_0 specimen has the largest amount of oxide film. With increasing the Mo content, the amount of oxide film in EHEAs is firstly decreased and then maintained at a certain level. When the Mo content increases from 0at% to 4at%, the amount of oxide film decreases; when the Mo content increases from 4at% to 10at%, the amount of oxide film barely changes.

Fig. 7 shows SEM microstructures of the wear tracks of different $Al_{19}Fe_{20-x}Co_{20-x}Ni_{41}Mo_{2x}$ EHEAs. In Fig. 7, area A represents the exposed substrate caused by the peeling of oxide film; area B represents the thinner oxide film; area C represents the thicker oxide film. The wear tracks of EHEAs present the typical ploughing grooves and flake-shape wear debris, indicating the abrasive wear and delamination wear mechanisms, respectively. The oxides (white flakes with oxygen content>60at%) can be observed in all wear tracks of EHEAs. The oxidation is mainly caused by the temperature rise at the sliding interface between the ball and disk. Compared with the wear surface of Mo_0 EHEA specimen, less wear debris caused by delamination and less mixed oxides exist on the surface of Mo_4 EHEA specimen, indicating the better wear resistance of Mo_4 EHEA specimen[32]. With further increasing the Mo content, the amount of wear debris on the EHEA specimen surface is increased again. The fact that COF is decreased with increasing the Mo content is probably attributed to the better oxidation resistance caused by Mo addition and the formation of more protective tribo-oxide layer during friction and wear process. The wear resistance of Mo_4 EHEA improves, which is caused by the higher hardness of fcc+B2 near-eutectic microstructures and the formation of a more protective tribo-oxide layer during sliding process. With further increasing the Mo content, the wear resistance is decreased due to the appearance of μ phase.

3 Conclusions

1) The Mo addition can significantly improve the yield strength and wear resistance of $Al_{19}Fe_{20}Co_{20}Ni_{41}$ eutectic high-entropy alloys (EHEAs).

2) With x=0–2, the $Al_{19}Fe_{20-x}Co_{20-x}Ni_{41}Mo_{2x}$ EHEAs show face-centered cubic (fcc) +B2 near-eutectic microstructures. With x=3–5, the $Al_{19}Fe_{20-x}Co_{20-x}Ni_{41}Mo_{2x}$ EHEAs present fcc+B2+μ dendritic microstructures.

3) The strength and plasticity simultaneously increase with minor Mo addition, whereas the plasticity significantly

decreases after the appearance of μ phase.

4) $Al_{19}Fe_{16}Co_{16}Ni_{41}Mo_8$ EHEA has good mechanical properties with fine wear resistance, which is attributed to the optimal addition of Mo element.

References

1 Lu Y P, Dong Y, Guo S *et al. Scientific Reports*[J], 2014, 4(1): 6200
2 Shi P, Ren W, Zheng T *et al. Nature Communications*[J], 2019, 10(1): 489
3 Li Y H, Yu T, Ye Y C *et al. Rare Metal Materials and Engineering*[J], 2021, 50(5): 1635
4 Kumar D. *Progress in Materials Science*[J], 2023, 136: 101106
5 Shukla S, Wang T H, Cotton S *et al. Scripta Materialia*[J], 2018, 156: 105
6 Jin X, Bi J, Zhang L *et al. Journal of Alloys and Compounds*[J], 2019, 770: 655
7 Lan L W, Zhang H W, Yang Z Y *et al. Journal of Materials Research and Technology*[J], 2023, 25: 6250
8 Peng Z, Luo Z B, Li B W *et al. Rare Metals*[J], 2022, 41(6): 2016
9 Shi P J, Li R G, Li Y *et al. Science*[J], 2021, 373(6557): 912
10 Miao J W, Liang H, Zhang A J *et al. Tribology International*[J], 2021, 153: 9
11 Vo T D, Tieu A K, Wexler D *et al. Tribology International*[J], 2023, 184: 19
12 Vo T D, Tran B, Tieu A K *et al. Tribology International*[J], 2021, 160: 16
13 Yu Y, He F, Qiao Z H *et al. Journal of Alloys and Compounds*[J], 2019, 775: 1376
14 Ren J, Zhang Y, Zhao D X *et al. Nature*[J], 2022, 608(7921): 62
15 Peng Z, Fan Z Z, Abdullah M R *et al. Materials*[J], 2023, 16(13): 13
16 Sui Q X, Wang Z, Wang J *et al. Journal of Alloys and Compounds*[J], 2022, 913: 12
17 Zhang J, Li J G, Jin T *et al. Materials Science and Engineering A*[J], 2010, 527(13–14): 3051
18 Darolia R, Lahrman D, Field R. *Scripta Metallurgica et Materialia*[J], 1992, 26(7): 1007
19 Liu C T, Horton J A. *Materials Science and Engineering A*[J], 1995, 192–193: 170
20 Peng Z, Sun J, Luan H W *et al. Intermetallics*[J], 2023, 155: 6
21 Li Q L, Lv S Y, Hu X W *et al. Intermetallics*[J], 2022, 151: 10
22 Yu Y, Wang J, Li J S *et al. Rare Metals*[J], 2022, 41(12): 4266
23 Gong P, Li F W, Deng L *et al. Journal of Alloys and Compounds*[J], 2020, 817: 9
24 Ding H P, Gong P, Chen W *et al. International Journal of Plasticity*[J], 2023, 169: 20
25 Cao C J, Wang Y F, Zhang C X *et al. Rare Metal Materials and Engineering*[J], 2023, 52(4): 1439
26 Peng Z, Chen Y, Yin G *et al. Fundamental Research*[J], 2022, 2: 764
27 Han C Y, Xu Y F, Zhang R H *et al. Rare Metal Materials and Engineering*[J], 2022, 51(2): 607
28 Zhang Y, Zhou Y J, Lin J P *et al. Advanced Engineering Materials*[J], 2008, 10(6): 534
29 Guo S, Ng C, Lu J *et al. Journal of Applied Physics*[J], 2011, 109(10): 5
30 Jia C C, Ishida K, Nishizawa T. *Metallurgical and Materials Transactions A*[J], 1994, 25(3): 473
31 Krbata M, Eckert M, Majerik J *et al. Metals*[J], 2020, 10(6): 16
32 Shen X J, Zhang C, Yang Y G *et al. Additive Manufacturing*[J], 2019, 25: 499

Mo添加对$Al_{19}Fe_{20-x}Co_{20-x}Ni_{41}Mo_{2x}$共晶高熵合金摩擦学性能的影响

彭　振[1]，郭庆宇[1]，孙　健[1]，李可然[2]，栾亨伟[3,4,5]，龚　攀[2,6]

(1. 江苏大学 材料科学与工程学院，江苏 镇江 212013)

(2. 华中科技大学 材料科学与工程学院，湖北 武汉 430074)

(3. 香港城市大学 机械工程系，香港 999077)

(4. 香港城市大学 国家贵金属材料工程技术研究中心香港分中心，香港 999077)

(5. 清华大学 材料学院，北京 100084)

(6. 深圳华中科技大学研究院，广东 深圳 518057)

摘　要：研究了$Al_{19}Fe_{20-x}Co_{20-x}Ni_{41}Mo_{2x}$（$x$=0，1，2，3，4，5）共晶高熵合金（EHEAs）的摩擦学性能。结果表明，添加微量Mo的EHEA可形成面心立方（fcc）+B2共晶组织，而添加相对较高含量Mo的EHEAs可形成fcc+B2+μ树枝状组织。Mo元素有利于提高$L1_2$相的强度和B2相的延性。然而，随着Mo含量的增加，生成的富Mo μ相降低了EHEAs的强度和塑性。$Al_{19}Fe_{18}Co_{18}Ni_{41}Mo_4$ EHEA具有高强度和高延展性的最佳组合。增加Mo含量可以提高EHEAs的抗氧化性。随着Mo含量的增加，EHEA在滑动过程中形成了抗氧化性增强的摩擦氧化物层，摩擦系数单调下降。本研究为$Al_{19}Fe_{20-x}Co_{20-x}Ni_{41}Mo_{2x}$ EHEAs的摩擦学性能研究提供了指导。

关键词：共晶高熵合金；摩擦学性能；强度；塑性

作者简介：彭　振，男，1981年生，博士，教授，江苏大学材料科学与工程学院，电话：0511-88780190，E-mail：peng@ujs.edu.cn